J. Fluid Mech. (2002), *vol.* 463, *pp.* 25–52.
DOI: 10.1017/S0022112002008698 Printed in the United Kingdom

On sound generation by the interaction between turbulence and a cascade of airfoils with non-uniform mean flow

By I. EVERS AND N. PEAKE

Department of Applied Mathematics and Theoretical Physics, University of Cambridge, Silver Street, Cambridge CB3 9EW, UK

(Received 4 September 2000 and in revised form 23 January 2002)

The sound generated by the interaction between a turbulent rotor wake and a stator is modelled by considering the gust response of a cascade of blades in non-uniform, subsonic mean flow. Previous work by Hanson & Horan (1998) that considers a cascade of flat plates at zero incidence is extended to take into account blade geometry and angle of attack. Our approach is based on the work of Peake & Kerschen (1997), who calculate the forward radiation due to the interaction between a single vortical gust and a cascade of flat plates at non-zero angle of attack. The extensions completed in this present paper are two-fold: first we include the effects of small but non-zero camber and thickness; and second we produce uniformly valid approximations which predict the upstream radiation near modal cut-off. The thin-airfoil singularity in the steady flow at each leading edge is crucial in our model of the sound generation. A new analytical expression for the coefficient of this singularity is derived via a sequence of conformal mappings, and it turns out that in our asymptotic limit this is the only quantity which needs to be calculated from the steady flow in order to predict time-averaged noise levels. Once the response to a single gust has been completed, we use Hanson & Horan (1998)'s approach to determine the response to an incident turbulent spectrum, and find that as well as the noise corresponding to the auto-correlation of the gust velocity component normal to the blade, there is also a contribution from the cross-correlation of the normal and tangential velocities. Predictions are made of the effects of blade geometry on the upstream acoustic power level. The blade geometry can have a very significant effect on the noise generated by interaction with a single gust, with changes of up to 10 dB from the flat-plate noise levels. However, once these gust results have been integrated over a full incident turbulence spectrum the effects of the geometry are rather smaller, although still potentially significant, leading to changes of up to about 2 dB from the flat-plate results. The implication of all this is that the blade geometry can have a significant effect on the tonal noise components generated by rotor–stator interaction (i.e. by single harmonic gusts), but that the broadband part of the noise spectrum is relatively unaffected.

1. Introduction

The interaction between the (turbulent) rotor wake and downstream stator blades is a primary source of both tonal and broadband noise in large aeroengines – see figure 1. Of most practical interest are situations involving high (subsonic) flow Mach numbers and large reduced frequencies, and in these cases the sound generation is

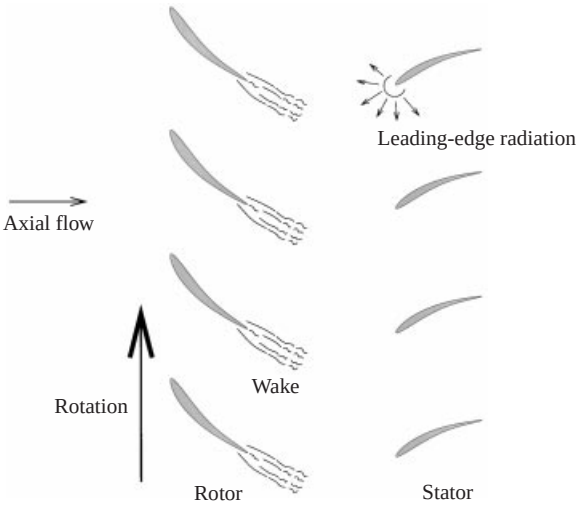

FIGURE 1. Rotor–stator interaction.

particularly sensitive to the effects of the stator-blade thickness, camber and angle of attack and the corresponding mean-flow non-uniformities. Our aim here is therefore to predict the upstream noise produced by the interaction between a spectrum of convected vorticity waves and a cascade of airfoils, taking full and systematic account of the effects of the blade geometry.

The analysis to be described here extends previous work in several ways. A number of previous analyses have considered single convected gusts interacting with cascades of flat plates aligned with the uniform oncoming flow, using the Wiener–Hopf technique (e.g. Mani & Horvay 1970 and Koch 1971, while Peake 1992 derived simplifications of the Wiener–Hopf factorization in the high-frequency limit). Hanson & Horan (1998) consider specifically the broadband noise caused by the interaction between a full spectrum of turbulence and a flat-plate cascade, using the numerical approach of Smith (1972) to determine the response to each gust component.

For numerical solutions of the full unsteady Euler equations we refer to the review by Verdon (1993). More analytically based investigations often involve the use of Goldstein's (1978) extension of the classical rapid distortion theory (Batchelor & Proudman 1954), and this is the approach which will be adopted here. The unsteady disturbances are taken to be small and the inviscid-flow equations are linearized about a compressible, irrotational mean flow, resulting in an inhomogeneous convected wave equation with variable coefficients in the wave operator. The source term and the coefficients depend on the mean flow and account for acoustic volume sources and for the influence of mean-flow gradients on the acoustic propagation. Numerical solution of this equation has been undertaken by Atassi and coworkers (see for instance Atassi, Subramaniam & Scott 1990). Alternatively, an asymptotic analysis in the limit of large reduced frequency, k, has been completed by Myers & Kerschen (1995) to model the gust–blade interaction for a single flat plate at a small angle of attack to oncoming subsonic flow, while Tsai & Kerschen (1990) and Myers & Kerschen (1997) performed similar studies to determine the additional effects of small thickness and camber. These asymptotic calculations turn out to be equivalent to singular perturbation analysis in which sound generation takes place in an inner region around the airfoil leading edge, with geometric-acoustics propagation in the

outer region. This demonstrates that at high frequency the noise generation may effectively be described by acoustic point sources at the leading edge, and that any other sources, specifically those at the trailing edge, along the airfoil surface and along the wake, are asymptotically smaller. The robustness of the high-frequency approximation is well-established (see Amiet 1976, and others), and this is especially the case for increasing Mach numbers, for which the acoustic reduced frequency is increased.

Peake & Kerschen (1997) combined the Myers & Kerschen (1995) work with earlier results for the cascade in a uniform stream (Peake 1992) to predict the upstream noise generated by a cascade of flat plates at non-zero angle of attack. Our first aim in the current paper is to include the effects of airfoil thickness and camber in this analysis. The second extension we present here concerns the type of disturbance that impinges on the stator vanes to produce sound (see figure 1). Whereas Peake & Kerschen (1997) consider single harmonic vortical gusts, here we integrate a spectrum of such incident waves to describe the rotor-wake turbulence. In doing this we are extending the work of Hanson & Horan (1998) to include the effects of stator blade geometry. In uniform flow only the normal velocity can generate noise (due to momentum blocking by the blade), but once non-uniform flow is included the tangential component of the incident gust velocity can also generate noise (in part by producing an unsteady stress close to the airfoil nose). This leads to an additional source of broadband noise, which is not present in the work of Hanson & Horan (1998), as well as contributing to the tonal noise generated by single gust components. A difficulty which arises immediately when trying to predict the cascade response, however, is that the amplitudes of the plane-wave modes, as presented in Peake & Kerschen (1997), are only valid when the modes are well cut-on and become singular as the modes approach cut-off. In the cascade response to a complete turbulence spectrum, it is inevitable that some modes generated are close to cut-off, and a uniformly valid solution which predicts finite amplitudes for all possible values of the relevant parameters will therefore be required. Peake & Kerschen (1995) derive such a solution for the flat-plate cascade, and another aim of the present work is therefore to extend that analysis to include the effects of non-uniform flow.

Determination of the steady flow can be completed in the context of thin-airfoil theory using a pair of conformal mappings which map the cascade onto a single airfoil. The effective incidence angle of the steady flow near each leading edge (which differs from the angle of attack relative to the upstream flow due to the turning effect of the cascade) is required for subsequent acoustic calculations, and analytical expressions for this have been derived from the conformal mapping and are presented in § 2. Indeed, the effective incidence angle is the only parameter which needs to be calculated when one wants to predict time-averaged measures of the acoustic level, as is usually done in practice and as is done throughout this paper. Prediction of the full phase of the upstream radiation requires an expression for the complex disturbance potential at upstream infinity, which can also easily be calculated from our conformal mappings (see Evers 1999 for full details). The extension of the acoustic analysis of Peake & Kerschen (1997) to include blade thickness and camber for a single incident gust is described in § 3, with sample results showing the very significant effects which this can have on the noise. However, these results become singular close to modal cut-off, and in § 4 we describe how they can be rendered uniformly valid. Finally, in § 5 we show, following Hanson & Horan (1998), how the response to a single gust can be used to predict the broadband noise produced by a full turbulence spectrum.

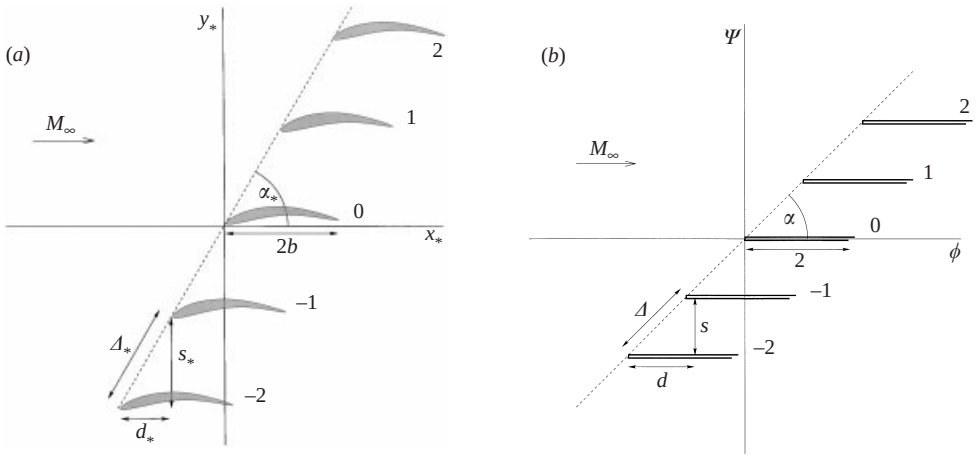

FIGURE 2. The staggered cascade in (*a*) physical space, and (*b*) (ϕ, ψ)-space.

2. Mean flow

2.1. *Steady formulation*

We consider a two-dimensional linear cascade of blades, as shown in figure 2(*a*). The blades are numbered from $-\infty$ to ∞, and the leading edge of the zeroth blade is fixed at the origin of the (x_*, y_*) coordinate system. The blades are regularly spaced, with leading-edge separation Δ_* and stagger angle α_*, equivalent to leading-edge separations d_* along the x_*-axis and s_* along the y_*-axis, so that $\tan\alpha_* = s_*/d_*$. The upstream steady flow is aligned parallel with the x_*-axis, with subsonic speed U_∞ (Mach number $M_\infty < 1$). The upper and lower surfaces of blade zero are $y_* = \delta b_* N^{\pm}(x_*)$ for $0 < x_* < 2b_*$, where b_* is the airfoil semi-chord. The functions $N^{\pm}(x_*)$ describe the blade thickness and camber distributions and the inclination to the oncoming flow. We will suppose that $\delta \ll 1$, as is standard in thin-airfoil theory. We also suppose that $N^{\pm}(x_*) \sim \pm(2Rx_*/b_*)^{1/2}$ as $x_* \downarrow 0$, so that the blades have a parabolic leading edge of radius $Rb_*\delta^2$. Note that in order to be able to treat the steady mean flow as being strictly subsonic, we will require $1 - M_\infty < O(\delta^{2/3})$. For transonic values of M_∞, the sort of analysis described in Evers & Peake (2000) would be required.

We introduce the Prandtl–Glauert transformation $x = x_*/b_*$ and $y = \beta_\infty y_*/b_*$, where $\beta_\infty = (1 - M_\infty^2)^{1/2}$. The horizontal leading edge separation is normalized to $d = d_*/b_*$, while the vertical separation transforms to $s = \beta_\infty s_*/b_*$. Accordingly, Δ_* and α_* are replaced by

$$\Delta = (d_*^2 + \beta_\infty^2 s_*^2)^{1/2}/b_* \quad \text{and} \quad \alpha = \tan^{-1}(\beta_\infty \tan\alpha_*), \tag{2.1}$$

respectively. As in Peake & Kerschen (1997), we use the dimensional potential and streamfunction for the steady flow, ϕ_* and ψ_*, to define the new coordinates

$$\phi = \frac{\phi_*}{U_\infty b} \quad \text{and} \quad \psi = \frac{\beta_\infty \psi_*}{U_\infty b}, \tag{2.2}$$

and it follows that

$$\zeta \equiv \phi + \mathrm{i}\psi = \zeta_0 + \delta F(\zeta_0) + O(\delta^2), \tag{2.3}$$

where $\zeta_0 = x + \mathrm{i}y$ and $\delta b_* U_\infty F$ is the complex disturbance potential for the steady flow. To $O(\delta)$ accuracy the transformation to (ϕ, ψ)-space can be written as the Prandtl–

Glauert transformation, $\phi = x_*/b + O(\delta)$ and $\psi = \beta_\infty y_*/b + O(\delta)$, and the disturbance potential can be expressed in the new coordinates according to $F(\zeta_0) = F(\zeta) + O(\delta)$, where $\zeta = \phi + \mathrm{i}\psi$. Our choice of the arbitrary constant associated with the complex potential leaves $F(0) = 0$, and it turns out that F consequently disappears at the leading edge of every blade. The cascade in physical space is mapped onto a cascade of straight-line segments in (ϕ, ψ)-space, with stagger α and leading-edge separation Δ – see figure 2(*b*).

The steady disturbance flow is related to the equivalent incompressible complex potential, F_i, according to $F = F_i/\beta_\infty$. To determine F_i, the usual rigid-surface boundary condition is applied along the chord line of each blade, consistent with the small-disturbance approximation $\delta \ll 1$, and requires

$$-\mathrm{Im}\left(\frac{\mathrm{d}F_i}{\mathrm{d}\zeta_0}(x)\right) = \frac{\mathrm{d}N^{\pm}}{\mathrm{d}x}(x) \quad nd \leqslant x \leqslant nd + 2 \quad \text{on } y = ns, \tag{2.4}$$

on each blade n. Far upstream and downstream we require that $\mathrm{d}F_i/\mathrm{d}\zeta_0 \to 0$ and $\mathrm{d}F_i/\mathrm{d}\zeta_0 \to$ const. as $\zeta_0 \to \mp\infty$ respectively, where the latter condition corresponds to the $O(\delta)$ deflection of the oncoming flow by the cascade. The Kutta condition at the blade trailing edges must also be enforced. In the next subsection we show how the steady flow can be calculated, and in particular we develop an analytical expression for the quantity which is required in subsequent acoustic calculations, namely the strength of the flow near the blade leading edges.

2.2. *Conformal mapping for steady flow*

There are essentially two different approaches to the determination of the cascade steady flow. First, transformation methods use one or a series of conformal transformations that map the cascade onto simpler geometries with known flow potentials. For instance, there is an exact transformation of a staggered cascade of zero-thickness flat plates onto the circle (Grammel 1917; Robinson & Laurmann 1956). Merchant & Collar (1941) show how the flow through a cascade of blades that resemble Joukowski airfoils is related to that past a series of ovals, while others examine flows through cascades of arbitrary airfoils using transformations onto the circle similar to Theodorson's transformation (e.g. Carter & Hughes 1946; Hall & Thwaites 1962). These methods involve approximation errors resulting from the necessary truncation of the infinite series of the conformal mapping functions, and particularly around the blade leading edge the convergence of the transformation series can be poor. Goto & Shirakura (1982) avoid this latter problem by choosing a conformal transformation to a cascade of circles rather than to a single circle. However, the potential for the circles, as well as the transformation itself, are in the form of series approximations, and the leading-edge behaviour cannot easily be extracted.

Second, in the method of singularities the flow is modelled by distributing sources and vortices along the chord or mean line for thin blades (Mellor 1959), or along the surface for thick blades (Martensen 1971). In a modification of Schlichting (1955), Mellor (1959) derives closed-form expressions for the velocity field induced by a cascade of thin blades in terms of an infinite summation of triple integrals involving the blade shape. Martensen (1971) uses a distribution of vortices around the profile to obtain integral equations for the flow potential which are well-suited to numerical solution. Indeed, the use of singularity distributions around the blade surface is appropriate for numerical investigations of the flow problem for thick blades, but is numerically unstable for thin blades and in any event does not yield convenient closed-form expressions for the leading-edge flow.

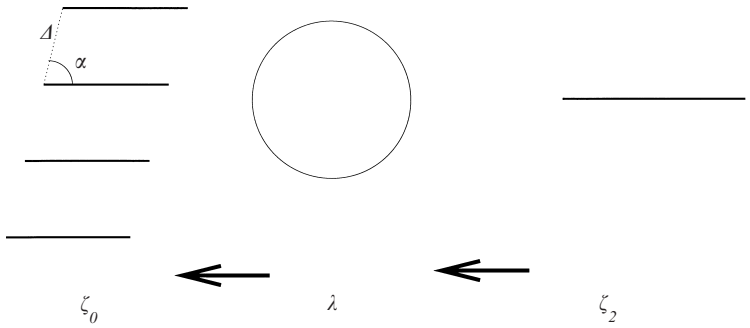

FIGURE 3. The series of conformal mappings used to calculate the steady flow.

In this subsection we indicate how a combination of the methods of conformal mappings and singularity distributions can be used to provide an analytical expression for the steady flow near the leading edges, which is exact within the context of thin-airfoil theory and which can be calculated trivially. Our starting point is the conformal transformation of the cascade in the ζ_0-plane onto a single airfoil in the ζ_2-plane. Robinson & Laurmann (1956, p. 149, equation 2.11,12) describe a transformation of a cascade of chord lines onto a circle in some complex space $\lambda \equiv \exp(\mathrm{i}\vartheta)$, and a second transformation of this circle onto a single airfoil can be achieved by taking the blade separation in the inverse of this first transformation to infinity. Combining these transformations, we find the conformal mapping $\zeta_0 = \Lambda(\zeta_2) \equiv \bar{\Lambda}(\vartheta(\zeta_2))$, where $\vartheta(\zeta_2) = \arccos(1-\zeta_2)$ and

$$\bar{\Lambda}(\vartheta) = 1 + \frac{d}{\pi}\tan^{-1}\left\{\frac{2\tau\sin(\vartheta-\theta^*)}{\tau^2-1}\right\} - \frac{s}{\pi}\tanh^{-1}\left\{\frac{2\tau\cos(\vartheta-\theta^*)}{\tau^2+1}\right\}. \tag{2.5}$$

Here the real constant $\tau > 1$ is obtained from

$$\frac{\Delta}{\pi}\left\{\sin\alpha\sinh^{-1}\left(\frac{2\tau\sin\alpha}{\tau^2-1}\right) + \cos\alpha\sin^{-1}\left(\frac{2\tau\cos\alpha}{\tau^2+1}\right)\right\} = 1, \tag{2.6}$$

while

$$\theta^* = \tan^{-1}\left\{\left(\frac{\tau^2-1}{\tau^2+1}\right)\cot\alpha\right\}. \tag{2.7}$$

The leading and trailing edges of the single airfoil, $\zeta_2 = 0$ and $\zeta_2 = 2$, are given by $\vartheta = 0$ and $\vartheta = \pi$ respectively, and the upper and lower halves of the circle in the λ-plane, given by $0 \leqslant \mathrm{Re}(\vartheta) < \pi$ and $\pi \leqslant \mathrm{Re}(\vartheta) < 2\pi$ (both with $\mathrm{Im}\,\vartheta = 0$), map to the upper and lower surfaces of the single airfoil in the ζ_2-plane. In general two points on either side of a cascade blade with the same coordinate $\mathrm{Re}(\zeta_0)$ map to two points on either side of the single airfoil in the ζ_2-plane with different coordinates $\mathrm{Re}(\zeta_2)$. This will be of importance when we determine $N_2^{\pm}$, the profile of the single airfoil in the ζ_2-plane. A diagram demonstrating the sequence of conformal mappings used is shown in figure 3.

The total disturbance potential of the cascade in incompressible flow, F_i, is written in the form $F_i = F_2 + F_c$, where F_2 is the disturbance potential of the single airfoil in the ζ_2-plane. The contribution F_c arises because points at infinity in the ζ_2-plane are not mapped to points at infinity in the ζ_0-plane, leading to inadmissible singularities in the flow domain between the blades at $\zeta_0 = 1 + (j+1/2)\Delta\exp(\mathrm{i}\alpha)$ for all integers j. These are removed by adding a row of discrete vortices of, at this stage unknown, strength Γ, which then account for the total circulation per blade (i.e. the potential F_2 of the

isolated airfoil does not contribute to the circulation in ζ_0-space). This circulation induces a non-zero flow far upstream with a complex potential that behaves like $\Gamma \exp(-i\alpha)\zeta_0/2\Delta$ as $\zeta_0 \to -\infty$. In order to satisfy our far-field boundary condition (that the disturbance to the uniform oncoming flow disappear far upstream) this term must be subtracted from our solution. The complex potential F_c that cancels the transformation singularities yet has the correct upstream behaviour is therefore

$$F_c(\zeta_0) = \frac{i\Gamma}{2\pi} \log\left\{1 + \exp\left(\frac{2\pi i}{\Delta} e^{-i\alpha}(\zeta_0 - 1)\right)\right\} - \frac{i\Gamma}{2\pi} \log\left\{1 + \exp\left(-\frac{2\pi i}{\Delta} e^{-i\alpha}\right)\right\}. \quad (2.8)$$

In this formulation, $F_c(0) = 0$ and the logarithmic branch cuts are straight lines that extend downstream from the singularities in the direction normal to the face of the cascade. The (normalized) circulation Γ is at this stage unknown but will depend, through (2.12), on the profile function $N_2^{\pm}$, which we determine next.

2.3. *Solution for steady flow*

In order to determine the disturbance potential for the single airfoil, F_2, we need to determine the effective boundary condition to be applied in ζ_2-space, equivalent to specifying the single-airfoil surface $N_2^{\pm}$. The boundary condition for the single-airfoil flow that is consistent with the cascade problem is found by substituting the cascade disturbance potential, $F_i(\zeta_0) = F_2(\Lambda^{-1}(\zeta_0)) + F_c(\zeta_0)$, into (2.4) and expressing the result in ζ_2-space. It proves convenient to define the odd and even parts of the single-airfoil surfaces by $N_{2o} = (N_2^+ + N_2^-)/2$ and $N_{2e} = (N_2^+ - N_2^-)/2$ respectively, and it turns out that

$$\frac{dN_{2o,2e}}{dx_2}(\theta) = \frac{1}{2}\left[\frac{dN^+}{dx} + (A_0 - A_1)V_c\right]\left(\bar{\Lambda}(\theta)\right)\frac{d\bar{\Lambda}}{d\zeta_2}(\theta) \pm \frac{1}{2}\left[\frac{dN^-}{dx} + \frac{\Gamma}{\pi}V_c\right]\left(\bar{\Lambda}(-\theta)\right)\frac{d\bar{\Lambda}}{d\zeta_2}(-\theta), \quad (2.9)$$

where

$$V_c(\zeta_0) \equiv \frac{\pi}{\Gamma}\mathrm{Im}\left(\frac{dF_c}{d\zeta_0}(\zeta_0)\right) = \frac{\pi}{2\Delta}\mathrm{Re}\left\{e^{-i\alpha}\tan\left(\frac{\pi}{\Delta}e^{-i\alpha}(\zeta_0 - 1)\right)\right\} - \frac{\pi}{2\Delta}\sin\alpha. \quad (2.10)$$

Here $\theta = \arccos(1 - x_2)$ on the blade surface (where $x_2 = \mathrm{Re}(\zeta_2)$). Equation (2.9) does not correspond to the odd and even parts of the blade profiles in physical space, because $\bar{\Lambda}(-\theta) \neq \bar{\Lambda}(\theta)$ in general. Consequently, there can exist an antisymmetric cascade flow (and a corresponding non-zero lift) even when the blades are symmetric and the angle of attack is zero, but only when the cascade is staggered.

Determination of the disturbance potential for a thin isolated airfoil of prescribed shape is completed in a standard fashion by introducing distributions of point vortices (corresponding to the odd part of the shape distribution N_{2o}) and mass sources (corresponding to the even part N_{2e}) on the airfoil chord. For instance, one writes the vortex strength per unit chordwise distance as

$$\gamma(\theta) = -A_0 \cot(\theta/2) + 2\sum_{n=1}^{\infty} A_n \sin n\theta, \quad (2.11)$$

accounting for the lift-induced flow. Note that the first term on the right-hand side of (2.11) accounts for the leading-edge singularity (as $\theta \to 0$), which is a feature of thin-airfoil theory, so that A_0 is proportional to the strength of the leading-edge

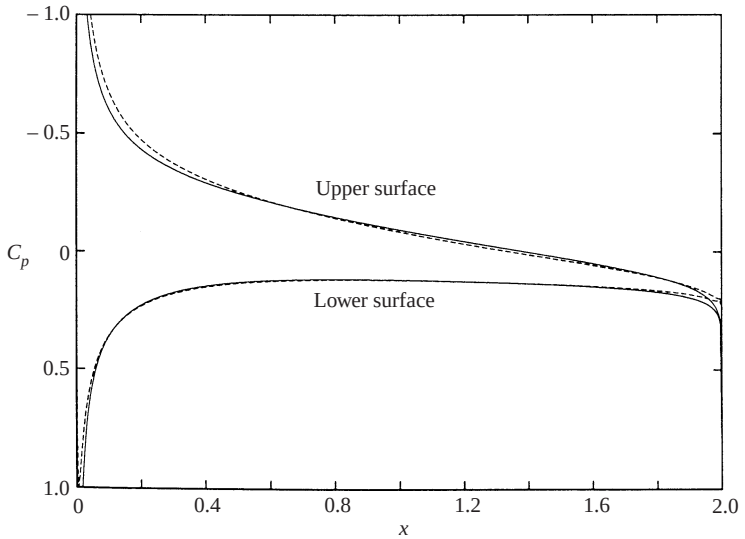

FIGURE 4. Pressure coefficient for a cascade of NACA0005 airfoils with 6° angle of attack, using the current thin-airfoil theory (solid line) and a numerical solution (dashed). Here, $\alpha = 45°$, $\Delta = 3$ and the flow is assumed incompressible.

vortex introduced to model this singularity. The Fourier coefficients are given by

$$A_n = \frac{2}{\pi}\int_0^\pi N'_{2o}(\theta)\cos n\theta \,\mathrm{d}\theta, \quad n = 0, 1, 2, \ldots \tag{2.12}$$

(see Houghton & Carruthers 1982, for example). Similarly, the thickness-induced mass source terms can also be written as a Fourier series, with coefficients B_n say. Both sets of Fourier coefficients can be calculated by substituting (2.9) into (2.12), and into the equivalent result for the B_n, and once all the Fourier coefficients are known the full disturbance complex potential $F_2(\zeta_2)$ can be recovered using standard results for the complex potential of simple sources. However, for the purposes of the acoustic calculations to follow it turns out that we only need to know A_0 and A_1, and after considerable but straightforward algebra it turns out that

$$\begin{pmatrix} A_0 \\ A_1 \end{pmatrix} = \frac{1}{1 + \mathscr{A}_1(V_c) - \mathscr{A}_0(V_c)} \begin{pmatrix} 1 + \mathscr{A}_1(V_c) & -\mathscr{A}_0(V_c) \\ \mathscr{A}_1(V_c) & 1 - \mathscr{A}_0(V_c) \end{pmatrix} \begin{pmatrix} \mathscr{A}_0(\mathrm{d}N^+/\mathrm{d}x, \mathrm{d}N^-/\mathrm{d}x) \\ \mathscr{A}_1(\mathrm{d}N^+/\mathrm{d}x, \mathrm{d}N^-/\mathrm{d}x) \end{pmatrix}, \tag{2.13}$$

where we use the notation

$$\mathscr{A}_n(f, g) = \frac{1}{\pi}\int_0^\pi \left[f\left(\bar{\Lambda}(\theta)\right) \frac{\mathrm{d}\bar{\Lambda}}{\mathrm{d}z_2}(\theta) + g(\bar{\Lambda}(-\theta)) \frac{\mathrm{d}\bar{\Lambda}}{\mathrm{d}z_2}(-\theta) \right] \cos n\theta \,\mathrm{d}\theta \tag{2.14}$$

for functions $f, g : [0, 2] \to \mathbb{R}$, with $\mathscr{A}_{0,1}(f) \equiv \mathscr{A}_{0,1}(f, f)$. The remaining coefficients A_n and B_n are given explicitly by single integrals of functions of the blade slopes, and could be determined in a similar manner. Full details of these calculations are given in Evers (1999), but in order to demonstrate the accuracy of our thin-airfoil approximation here a comparison is made with a numerical solution in figure 4. The

numerical solution is found from the panel method introduced by Martensen (1959), implemented according to Lewis (1991), in which vortices are distributed along the genuine cascade blade surfaces and their strengths determined by specifying zero velocity across the profile boundaries.

It can be shown that the blade circulation Γ is given by $\Gamma = \pi(A_0 - A_1)$. As stated in the previous paragraph, the steady flow within $O(\delta)$ of the leading edge of each blade is crucial to the acoustics which follow. Writing the total complex disturbance potential F as a sum of odd (F_o, lift-induced) and even (F_e, thickness induced) parts, it can be shown that near the leading edge of blade zero, i.e. as $\zeta \to 0$, we have

$$F \equiv F_o + F_e \sim \frac{2^{3/2} L \zeta^{1/2}}{\beta_\infty} - \frac{\mathrm{i}(2R)^{1/2}\zeta^{1/2}}{\beta_\infty}, \tag{2.15}$$

where

$$L = -\frac{A_0(\tau^2 - 1)\pi^{1/2}}{2(2\Delta\tau)^{1/2}(\tau^2 + 1)^{1/2}} \left(\frac{\cos\theta^*}{\sin\alpha}\right)^{3/2}, \tag{2.16}$$

and we recall that the parabolic leading edge of each blade has radius $Rb_*\delta^2$. We point out that the symmetric component of the leading-order velocity potential depends only on the local radius of curvature, and not on the profile shape further downstream nor on the cascade (which have an effect at higher order in δ and on higher terms in the expansion about $\zeta = 0$). The effects of the cascade enter the leading-edge region through the antisymmetric part of the flow, and we recall that A_0 is proportional to the strength of the vortex which models the thin-airfoil leading-edge singularity. The effective incidence angle of the steady flow onto the blade leading edges is in fact L/β_∞, where the usual Prandtl–Glauert factor accounts for the effects of compressibility. This angle is smaller than the angle of attack to the far upstream flow, due to the turning effect of the cascade. We emphasize that we have determined an analytical expression for L here, and it will turn out that the value of L is the only information about the steady flow which needs to be calculated in order to predict the upstream acoustic energy flux.

Our thin-airfoil theory breaks down in a region whose size scales on the airfoil nose radius around the leading-edge stagnation point of each blade, i.e. regions of size $O(\delta^2)$. Here the flow can no longer be considered to be a small perturbation to the uniform stream, and our linearization of the steady flow and the Prandtl–Glauert transformation are therefore invalid within $O(\delta^2)$ of a leading-edge stagnation point. In this paper we will be concerned with unsteady disturbances which have wavelength of size $O(\delta)$, and in particular we will be concerned with matching what we will call the *inner* region, of size $O(\delta)$ around the leading edge, onto the outer flow. It follows that thin-airfoil theory will be valid throughout this inner region, apart from in the small *inner-inner* region of size $O(\delta^2)$ around the stagnation point. This inner-inner region does not affect the asymptotic matching to the order to be considered in this paper, although of course it could well become important at higher order, or if one were to consider gust interaction with a bluff body in which the nose radius is $O(\delta)$, rather than the $O(\delta^2)$ value assumed in thin-airfoil theory. The result that the disturbance potential $F(\zeta)$ is proportional to $\zeta^{1/2}$ close to each leading edge (see equation (2.15)) is a direct consequence of thin-airfoil theory, and following the above remarks can be used in determining the gust interaction in the inner region. One consequence of (2.15) is then that the phase distortion experienced by any gust approaching the stagnation point will remain bounded as it passes through our inner region. It is well-known that the phase distortion of a convected gust diverges logarithmically as the gust

approaches a stagnation point (see Atassi & Grzedzinski 1989), but this divergence occurs within a region of size $O(\delta^2)$ around the leading edge, and therefore again does not affect our asymptotic approximation of the gust–airfoil interaction in the $O(\delta)$ inner region.

3. Unsteady response to a harmonic gust

3.1. *Single airfoil*

We proceed as in Peake & Kerschen (1997) and introduce the convected disturbances as vortical harmonic waves of frequency ω. We consider these waves to be Fourier components of the incident turbulence field, which will be calculated in § 5. Upstream we thus consider the unsteady velocity component $\boldsymbol{v}'$ in the form

$$\boldsymbol{v}' = \epsilon U_\infty (A_t, A_n, A_z) \mathrm{e}^{\mathrm{i}k(\phi + k_n \psi + k_3 z) - \mathrm{i}\omega t} \quad \text{as} \quad \phi \to -\infty, \tag{3.1}$$

where $k = \omega b / U_\infty$ is the aerodynamic reduced frequency and $z = z_*/b$ is the spanwise coordinate normalized by the semi-chord. The amplitudes A_t, A_n and A_3 of the gust components and the wavenumbers k_n and k_3 satisfy the condition $A_t + \beta_\infty k_n A_n + k_3 A_3 = 0$ for divergence-free flow far upstream. For the analysis that is presented here to be valid, we require $\epsilon \ll \delta \ll 1$, where ϵ is a measure of the amplitude of the unsteady flow. This allows the unsteady flow to be linearized about the non-uniform steady base flow, and implies that the forward stagnation point remains within a vanishingly small (i.e. $O(\delta^2)$) distance of the leading edge.

Based on Goldstein's convected wave equation (see Goldstein 1978), Myers & Kerschen (1995) construct a linear, asymptotic boundary-value problem for the modified unsteady potential $h(\phi, \psi)$, which is related to the physical potential $G'(\phi, \psi)$ of the unsteady flow by

$$G'(\phi, \psi) = \epsilon U_\infty b h(\phi, \psi) \exp[\mathrm{i}k(k_3 z - t - M_\infty^2 \phi / \beta_\infty^2) + M_\infty^2 \delta q]. \tag{3.2}$$

The dimensional steady flow speed is written as $U_\infty(1+\delta q)$, so that $q(\phi, \psi)$ corresponds to the perturbation to the upstream steady flow speed induced by the presence of the cascade. Kerschen & Myers (1986) show that h satisfies a wave equation of the form

$$(\mathscr{L}_0 + \delta \mathscr{L}_1)(h) = \delta k S(\phi, \psi) \exp(\mathrm{i}k\Omega), \tag{3.3}$$

where $\mathscr{L}_0 \equiv \nabla^2 + k^2 w^2$, and kw is the acoustic reduced frequency, with

$$w^2 = \left(\frac{M_\infty}{\beta_\infty^2} \right)^2 - \left(\frac{k_3}{\beta_\infty} \right)^2. \tag{3.4}$$

Equation (3.3) is an $O(\delta)$ perturbation to the Helmholtz equation, accounting for the non-uniform mean flow. Complicated expressions for the perturbation to the uniform-flow wave operator, $\delta \mathscr{L}_1$, and the perturbation source term, $\delta k S(\phi, \psi) \exp(\mathrm{i}k\Omega)$, are given by Myers & Kerschen (1995). In the asymptotic limits being considered, for large k and small δ, this source term can be neglected everywhere apart from close to the blade leading edge, where the mean-flow gradients are large. This means that the volume sources are located in the inner region, of size $O(\delta)$, around the leading edge, and arise from the local interaction between the gust and the mean-flow gradients. In uniform flow, sound is generated only by the blocking of unsteady gust momentum at the rigid blade surface, a process dominated for large kw by the leading edge, but for non-uniform flow this process is augmented by these volume sources. In the outer region, away from the leading edge, for large kw one is left to solve a ray tracing

problem through a medium which is almost uniform (i.e. with steady perturbations and flow gradients which are $O(\delta)$). The unsteady field generated in the inner region then matches onto a ray field in the outer region emanating from the leading edge. Full mathematical details behind these arguments are given in Myers & Kerschen (1997).

Neglecting for the moment the interaction between the leading-edge rays and other blades, it turns out that the radiation emitted from the leading edge of the zeroth blade in the cascade has modified potential $h_0(\phi, \psi)$ of the form

$$h_0(\phi, \psi) = \frac{D(\theta; A_N, A_t)}{k^{3/2} r^{1/2}} \exp[\mathrm{i}k(wr + \delta P(r, \theta) + \delta g_l)], \tag{3.5}$$

where $r = (\phi^2 + \psi^2)^{1/2}$ and $\theta = \tan^{-1}(\psi/\phi)$ are polar coordinates. δg_l represents the phase distortion, or drift, experienced by the gust in propagating from upstream infinity to the leading edge, and is given by $\delta g_l = 2\delta \mathrm{Re}[F(-\infty)]$ – see Myers & Kerschen (1995). (Note here that within the context of thin-airfoil theory δg_l is finite – see the discussion at the end of the previous section.) The phase distortion of the ray field due to its propagation through the non-uniform outer flow is represented by the function $P(r, \theta) = V(\theta)Q(r, \theta)$, where

$$V(\theta) = -\beta_\infty^2 w + \frac{(\gamma + 1)M_\infty^4}{2\beta_\infty^2 w} \left(\frac{1}{\beta_\infty^2} - w \cos\theta \right)^2, \tag{3.6}$$

$$Q(r, \theta) = \mathrm{Re}(\mathrm{e}^{-\mathrm{i}\theta} F(r\mathrm{e}^{\mathrm{i}\theta})). \tag{3.7}$$

This phase distortion can be obtained by seeking a ray solution of the homogeneous version of equation (3.3) in the outer region. In our preferred limit, the influence of mean-flow gradients on the phase in (3.5) is $O(k\delta) = O(1)$, and this will have a marked effect on amplitude terms of the forward radiation due to the various cascade effects. The directivity function $D(\theta; A_N, A_t)$ of equation (3.5) is the directivity for the radiation from the leading edge of a flat plate plus an $O(\delta k^{1/2})$ contribution that represents the effects of the symmetric and antisymmetric components of the non-uniform mean flow. This combination is determined by comparing the leading-edge flows of the thick, unloaded airflow studied in Tsai & Kerschen (1990) and the infinitely thin cambered and loaded airfoil studied in Myers & Kerschen (1995) with the leading-edge flow for our cascade (i.e. equation (2.15)). In this way we obtain

$$D(\theta; A_N, A_t) = D_0(\theta; A_N) + \delta k^{1/2}[LD_L(\theta; A_N, A_t) + R^{1/2} D_R(\theta; A_N, A_t)], \tag{3.8}$$

where

$$D_0(\theta; A_N) = \frac{A_n \mathrm{e}^{-\pi\mathrm{i}/4} \cos(\theta/2)}{\beta_\infty \pi^{1/2} (w \cos\theta - \beta_\infty^{-2})(w + \beta_\infty^{-2})^{1/2}} \tag{3.9}$$

is the leading-edge directivity of a flat plate in uniform flow, and the complicated functions D_L and D_R are taken from Myers & Kerschen (1995) (specifically $D_L = D_1 + D_2 + D_3$, given by their equations (3.11*b*), (3.15*b–e*) and (3.26*c*)) and Tsai & Kerschen (1990) ($D_t = K_1 + K_2 + K_3$, their equations 10b, 12b and 14b). It will be convenient to extract the (linear) dependence of the directivity on normal and streamwise gust amplitudes, A_N and A_t, by writing alternatively

$$D(\theta) = A_N D_N(\theta) + A_t D_t(\theta), \tag{3.10}$$

where $D_N(\theta) = D(\theta; 1, 0)$ and $D_t(\theta) = D(\theta; 0, 1)$. We note that $D_t(\theta) = O(\delta k^{1/2})$, corresponding to the fact that the tangential gust velocity can only generate noise in the presence of non-uniform mean flow.

In summary, the results presented here correspond to the first two terms in both the amplitude and phase of the noise produced by the interaction between an isolated airfoil and a gust. This has been completed in the limit $k \gg 1$, $\delta \ll 1$ with $k\delta = O(1)$. Implicit in this, however, has been the assumption that $kw \gg 1$ as well, which is required at various points in the analysis including the ray tracing in the outer region. Note that the condition $kw \gg 1$ can be violated when $k \gg 1$ is large if w is small, for instance if the Mach number is small.

3.2. *Cascade*

To determine the total radiation upstream of the cascade we need only consider the leading-edge sources described above because other sources, notably the scattering of the leading-edge field by the trailing-edge, see Peake & Kerschen (1997), are a factor $O(kw)^{-1}$ smaller than the leading-order solution. The total acoustic field upstream of the cascade can then be modelled using a row of isolated-airfoil ray fields centred on the blade leading edges. The sound from each leading edge can subsequently interact with other blades in the cascade, and Peake & Kerschen (1997) identify the following acoustic components that reach an upstream observer:

(i) The sound waves generated by the interaction between a gust and an individual blade, described by the ray field (3.5) for the zeroth blade, can travel directly upstream without interacting with any other blades. We refer to this as the direct field. The modified velocity potential of the direct field from leading edge zero is precisely $h_0(\phi, \psi)$, as given in the previous subsection. The quasi-periodicity of the cascade–gust interaction in the transverse direction means that the direct field from the nth leading edge is

$$h_n(\phi_n, \psi_n) = \mathrm{e}^{\mathrm{i}n\sigma'} h_0(\phi, \psi), \tag{3.11}$$

where $\phi_n = \phi - nd$ and $\psi_n = \phi - ns$ are potential-streamfunction coordinates centred on the nth leading edge. Here

$$\sigma' = \sigma + kM_\infty^2 d/\beta_\infty^2 \quad \text{and} \quad \sigma = k(d + k_n s). \tag{3.12}$$

The quasi-periodicity of the scattered field is a direct consequence of the fact that the incident gust imposes on the problem a wavenumber along the line of the leading edges, and (3.12) is obtained directly from (3.1) and (3.2). If r_n and θ_n are the polar coordinates centred on the nth leading edge, then the direct field from blade n reaches observers lying within $\alpha < \theta_n < \pi + \alpha$. The phase distortion a ray experiences in travelling directly from the nth leading edge to an observer in this sector far upstream, $k\delta p_1$ say, is given by the change in $k\delta P(r_n, \theta_n)$ over this distance, and since $P(0, \theta_n) = 0$ (because we have chosen $F(0) = 0$), we find

$$p_1(\theta_n) = P(\infty, \theta_n) = V(\theta_n)\,\mathrm{Re}(\mathrm{e}^{-\mathrm{i}\theta_n} F(-\infty)). \tag{3.13}$$

Here $F(-\infty)$ is obtained from the description of the steady field described in the previous section, and full analytical expressions are given in Evers (1999).

(ii) The direct field from each leading edge travels along the front face of the cascade and undergoes a complicated Fresnel-diffraction process as it interacts with all other blade leading edges. This interaction leads to more radiation being scattered upstream. To leading order in k, the radiation from blade 0 that reaches the leading edge of the nth blade is a fraction $1/n$ of the direct field that would have reached the nth blade had the intervening blades not been present (Peake & Kerschen 1997). If we consider the converse, namely the amount of radiation that reaches the zeroth blade from the nth leading edge, we conclude that this is proportional to $n^{-3/2}\Delta^{-1/2}$,

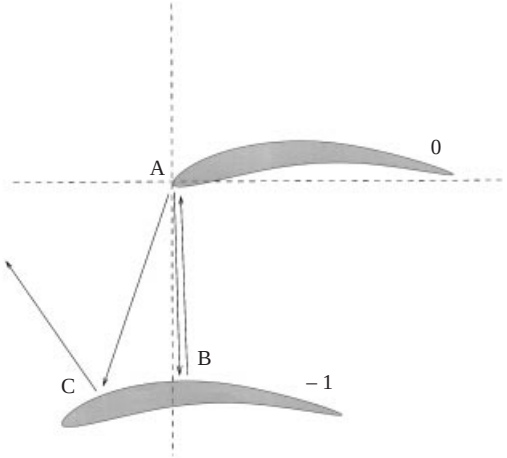

FIGURE 5. Reflections between blade n and blade $n-1$.

due to the cylindrical spreading of h_n. Since $F = 0$ at each blade leading edge, the field experiences no net phase distortion in propagating from one leading edge to another. A standard application of the Wiener–Hopf technique then gives the upstream radiation due to the rescattering of this incident field. This contribution to the upstream radiation is $O(k^{-1/2})$ smaller than the direct field, which means that in this rescattering problem the effects of local volume sources around leading edge zero can be neglected to the asymptotic order we consider.

(iii) In a staggered cascade the direct field from a given leading edge may be reflected arbitrarily many times by the adjacent lower blade before it is rescattered by the leading edge. Consider a ray that travels from a given leading edge (point A in figure 5) to the adjacent lower blade (point B) and back up to A. The phase distortion experienced by the ray over one complete reflection is denoted $k\delta p_2$, and by noting that B lies at $r_n = s$, $\theta_n = 3\pi/2$ and application of equation (3.6) it is easy to show that

$$p_2 = -2V(\pi/2)\,\mathrm{Im}(F(-\mathrm{i}s)). \tag{3.14}$$

The imaginary part of $F(\zeta)$ on the blade upper and lower surfaces is found by integrating the boundary condition (2.4) with respect to ϕ, giving $\mathrm{Im}(F(\phi \pm 0\mathrm{i})) = -N^{\pm}(\phi)/\beta_\infty$ on the upper and lower surfaces of blade n respectively, from which we find that

$$p_2 = \frac{2V(\pi/2)}{\beta_\infty} N^{+}(d). \tag{3.15}$$

The distortion $k\delta p_2$ is compounded for every reflection cycle, while the amplitude after the nth cycle decays like $n^{-3/2}(2s)^{-1/2}$. This latter point follows because the multiply reflected field is undergoing the same Fresnel process as quoted in point (ii) above for the decay of the direct field along the front face of the cascade; the multiply reflected field can be modelled as if being generated by a series of image sources at distances $2ns$ below the leading edge, and the fraction of the direct field which returns to the leading edge after n reflections by the lower blade is, to leading order in kw, $1/n$. Equation (3.15) is the generalization of equations (5.10) in Peake & Kerschen (1997) to include the effects of thickness and camber, and Peake & Kerschen's result is regained by setting $N^{+}(\phi) = -\phi$ to represent a flat-plate airfoil at non-zero incidence angle δ.

(iv) A ray of the direct field which travels at the angle $-\theta_n$ will be reflected by the adjacent lower blade and will propagate upstream if $\pi/2 < \theta_n < \pi - \alpha$ (e.g. the ray that reflects at point C in figure 5). The phase distortion experienced in travelling from A to the observer via C is denoted $k\delta[p_1(\theta_n) + p_3(\theta_n)]$, and in much the same way as was used to determined p_2 it follows that

$$p_3(\theta_n) = \frac{2}{\beta_\infty} V(\theta_n) N^+(\phi_C) \sin\theta_n, \tag{3.16}$$

where ϕ_C is the distance from the leading edge of blade $n-1$ to the point of reflection, specifically $\phi_C = s(\cot\alpha + \cot\theta_n)$. Equation (3.16) is the generalization of equation (5.12) in Peake & Kerschen (1997) to include the effects of thickness and camber, and once again their result can be regained by setting $N(\phi) = -\phi$.

The total radiation upstream is now determined by adding together the direct field (contribution i above) and the rescattered field, with the latter made up of contributions from the rescattering of other leading-edge fields by a given leading edge (contribution ii above) together with the multiple reflection by the adjacent blade (contribution iii above). Reflection of the total field from a given leading edge (contribution iv above) is also included. This leads to an infinite sum of cylindrically decaying fields, which can be converted into a summation of plane-wave modes via Poisson summation. In essence, the idea is that the radiation from the discrete row of point sources is written down in the form of an integral along the entire front face of the cascade, by use of an infinite series of delta functions in the integrand. Poisson's formula is then used to convert this series into an infinite series of plane waves, and then the method of stationary phase is used to approximate each integral, in the limit of large kw. Each element in the sum then corresponds to a plane-wave mode upstream of the cascade, only a finite number of which are cut on and therefore propagate to the far field. The details of this procedure are exactly as in the flat-plate case of Peake & Kerschen (1997), and need not be repeated here. We find that the upstream radiation takes the form

$$h \sim \sum_{n=n_r}^{n_q} R_n \exp[\mathrm{i}k(wr\cos(\theta - \theta_s^n) + \delta g_l + \delta p_1(\theta_s^n))], \tag{3.17}$$

where the angle of propagation of the nth mode is

$$\theta_s^n = \alpha + \arccos\left(\frac{\sigma' - 2n\pi}{\Delta kw}\right), \tag{3.18}$$

restricted to the angles $\alpha < \theta_s^n < \alpha + \pi$. Here the modal coefficients are given by

$$R_n = \frac{\mathrm{e}^{\pi\mathrm{i}/4}(2\pi)^{1/2}\mathscr{F}(\theta_s^n)}{\Delta k^2 w^{1/2}\sin(\theta_s^n - \alpha)}[A_N E_N(\theta_s^n) + A_t E_t(\theta_s^n)], \tag{3.19}$$

where

$$\begin{aligned} E_{N,t}(\theta_s^n) = {} & D_{N,t}(\theta_s^n) + \exp[2\mathrm{i}kws\sin\theta_s^n + \mathrm{i}k\delta p_3(\theta_s^n)] \\ & \times[\mathrm{H}(\theta_s^n - \pi/2) - \mathrm{H}(\theta_s^n - \pi + \alpha)]D_{N,t}(2\pi - \theta_s^n), \end{aligned} \tag{3.20}$$

$\mathrm{H}(\cdot)$ is the unit step function and $\mathscr{F}(\theta_s^n)$ is given by

$$\mathscr{F}(\theta_s^n) = 1 - \frac{\mathrm{i}(\tilde{M}\cos\theta_s^n - 1)}{\tilde{M}(kw)^{1/2}}\left(\frac{2^{1/2}\cos(\alpha/2)C_1}{\cos\theta_s^n + \cos\alpha} - \frac{2^{1/2}\sin(\alpha/2)C_2}{\cos\theta_s^n - \cos\alpha} - \frac{C_3}{\cos\theta_s^n}\right), \tag{3.21}$$

where

$$C_1 = \frac{\tilde{M}\mathrm{e}^{-\pi\mathrm{i}/4}\sin(\alpha/2)}{(\pi\Delta)^{1/2}(\tilde{M}\cos\alpha+1)}\sum_{m=1}^{\infty}\frac{\exp[\mathrm{i}(kw\Delta+\sigma')m]}{m^{3/2}}, \tag{3.22}$$

$$C_2 = \frac{\tilde{M}\mathrm{e}^{-\pi\mathrm{i}/4}\cos(\alpha/2)}{(\pi\Delta)^{1/2}(\tilde{M}\cos\alpha-1)}\sum_{m=1}^{\infty}\frac{\exp[\mathrm{i}(kw\Delta-\sigma')m]}{m^{3/2}}, \tag{3.23}$$

$$C_3 = \frac{\tilde{M}\mathrm{e}^{-\pi\mathrm{i}/4}}{2(\pi s)^{1/2}}\sum_{m=1}^{\infty}\frac{\exp[\mathrm{i}(2kws+k\delta p_2)m]}{m^{3/2}} \tag{3.24}$$

and $\tilde{M} = \beta_\infty^2 w = (M_\infty^2 - \beta_\infty^2 k_3^2)^{1/2}$, which satisfies $0 < \tilde{M} < 1$ for cut-on values of k_3. The C_1 term corresponds to the rescattering by blade n of the direct fields from blades $n+m, m = 1, 2, \ldots$, the C_2 term corresponds to the rescattering of the direct fields from blades $n-m$, $m = 1, 2, \ldots$ and the C_3 term corresponds to the multiple reflections of the direct field from blade n by blade $n-1$. That is, the terms $C_{1,2}$ correspond to contribution (ii) described earlier, while C_3 corresponds to contribution (iii).

The indices n_r and n_q are the lowest and highest integers n such that $|2n\pi-\sigma'| \leqslant \Delta kw$, so that any modes with indices inside this range are propagating and the modes outside are cut off. Note that the expression for R_n in equation (3.19) is singular when $\theta_s^n = \alpha,\ \pi+\alpha$, corresponding to that mode becoming cut off, and is also singular when $\theta_s^n = \pi/2,\ \pi-\alpha$ in equation (3.21), corresponding to the presence of the shadow boundary in contributions (iii) and (ii) respectively. The step functions in (3.20) show that mode angles in the range $\pi/2 < \theta_s^n < \pi-\alpha$ include contributions from the direct reflections (contribution iv).

The influence of blade geometry is contained in the higher-order components of the directivity function $D(\theta)$ and in the following phase terms. In (3.17), $k\delta g_l$ is the phase distortion experienced by the gust as it travels towards the cascade, while $k\delta p_1(\theta_n)$ is the distortion experienced by the acoustic waves that propagate upstream away from the cascade. Rays that are reflected by the blade surfaces into the region $\pi-\alpha \leqslant \theta \leqslant \pi/2$, which are represented by the second term on the right-hand side of (3.20), experience an additional distortion $k\delta p_3(\theta_n)$. Finally, the distortion associated with the bouncing mode, $k\delta p_2$, appears in the constant C_3.

3.3. *Sample results*

At this stage a numerical investigation of the results is restricted by the presence of singularities in the equations that correspond to cut-off conditions and shadow boundaries. We therefore fix a representative combination of admissible gust parameters so that the waves are well cut on and are well away from the shadow boundaries, allowing an examination of the influence of blade geometry on the acoustic response. For simplicity we assume that the gust is purely two-dimensional, so that $k_3 = A_3 = 0$. The gust wavenumbers are fixed by setting $k = 10$ and the inter-blade phase angle is $\sigma = 3\pi$. We also take $\alpha_* = \pi/4$, $\Delta_*/b_* = 3/2$ and $M_\infty = 0.5$. The remaining gust parameters A_t and A_n are then determined by the solenoidal condition and the normalization $A_t^2 + A_n^2 = 1$. In this case there are three cut-on modes upstream, with $n_r = 1$ and $n_q = 3$.

The time-averaged upstream energy flux per unit blade passage is $\rho_\infty U_\infty^3 b_* E$, and

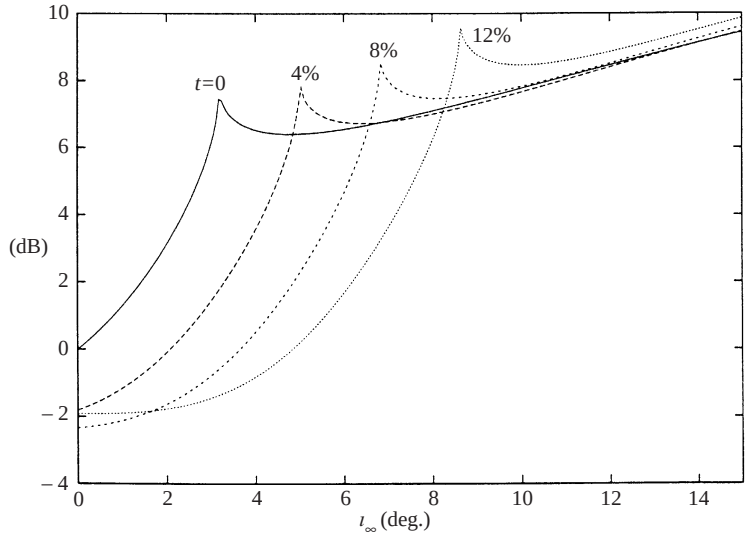

FIGURE 6. Normalized energy flux for a cascade of NACA 00XX blades for varying angle of attack.

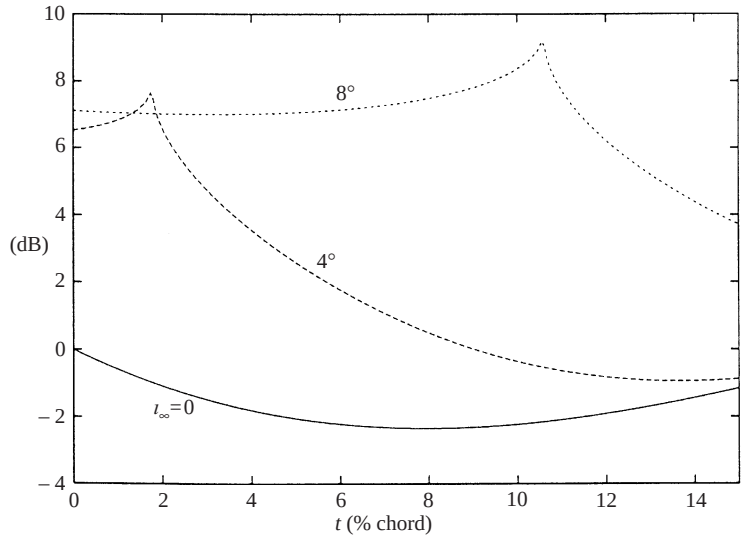

FIGURE 7. Normalized energy flux for a cascade of NACA 00XX blades at angle of attack for varying thickness.

an expression for E, given in Peake & Kerschen (1995), is

$$E = \frac{\Delta k^2 w \beta_\infty^2}{2} \sum_{n=n_r}^{n_q} \sin(\theta_s^n - \alpha)|R_n|^2. \tag{3.25}$$

It is easy to see that E is independent of both the drift $\delta k g_l$ and the direct-field phase distortion $\delta k p_1$, confirming that the value of $F(-\infty)$ from our steady-flow solution is not required. As a method of assessing the effects of the blade geometry on the noise, we plot the change in sound power level (i.e. $10 \log_{10} E$), with the flat-plate unloaded value of E taken as the reference level. In figures 6 and 7 we consider uncambered

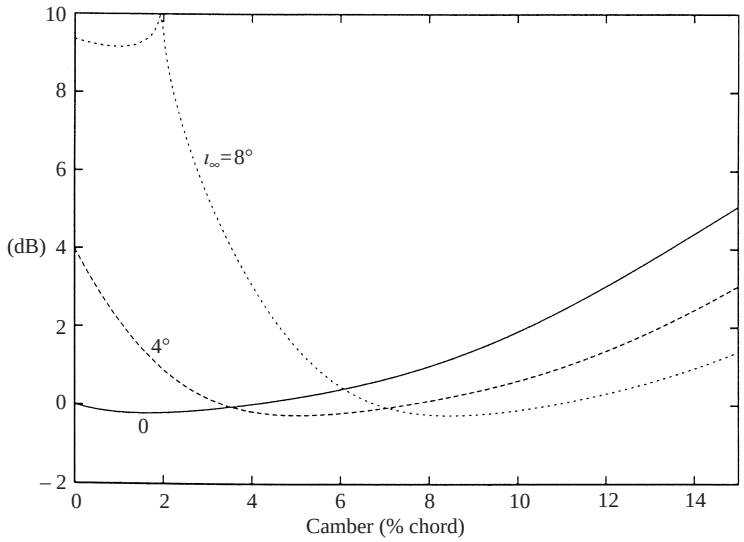

FIGURE 8. Normalized energy flux for a cascade of NACA X506 blades at angle of attack for varying camber.

NACA 00XX blades, with varying angle of attack for different blade thickness ratios, and with varying thickness ratios for different angles of attack respectively. It is clear that thickness and incidence can enhance as well as reduce the radiation, and changes to the intensity extend over more than 10 dB over the range considered. The effect of varying the camber of NACA four-digit sections is shown in figure 8, and significant changes on a decibel scale are again observed.

The significant effects seen in the figures 6–8 arise from the asymptotic corrections we have calculated. The correction to the amplitude of the radiation from a single blade is of size $O(\delta k^{1/2})$ compared to the flat-plate result. This is formally a small number, although in practical applications it may not be very small, but in any event it cannot account for the large decibel changes in the acoustic energy as the airfoil geometry is varied. The explanation for the large variations seen in figures 6–8 lies instead in the asymptotic correction to the phases of the various noise components, which is of size $O(k\delta)$ (and is therefore $O(1)$ in our preferred limit). Because the interference between many sources is a characteristic feature of cascade noise, it follows that these $O(1)$ phase corrections must have a big effect. For instance, if we consider just the leading-order directivity (i.e. without the $O(\delta k^{1/2})$ correction), it follows from equation (3.20) that the amplitude of an upstream mode is proportional to

$$|1 - \exp(2ikws \sin\theta_s^n + ik\delta p_3(\theta_s^n))|. \tag{3.26}$$

This represents the sum of the direct field from a given leading edge and the reflection of that field by the lower blade (provided that the mode angle satisfies $\pi/2 < \theta_s^n < \pi - \alpha$), and we recall that $p_3(\theta_s^n)$ is related to the extra mean-flow distortion experienced by the reflected ray. The direct and reflected fields will precisely cancel (total destructive interference), or add exactly in phase (total constructive interference), when the argument of the exponential in (3.26) is an even, or odd, integer multiple of πi respectively. This means that the amplitude of the upstream mode is zero, or

maximal, when the modal propagation angle satisfies

$$\theta_s^n = \sin^{-1}\left[\frac{N\pi - k\delta p_3(\theta_s^n)}{2kw}\right] \tag{3.27}$$

for integer N even, or odd, respectively. Hence, since $k\delta p_3(\theta_s^n) = O(1)$, it follows that the non-uniform mean flow can have the effect of making significant changes to the propagation angles along which the modes have zero, or maximal, amplitude. Most dramatically, if $k\delta p_3(\theta_s^n) > \pi$, it follows that there is the possibility of non-uniform mean flow causing what would have been a total destructive interference for uniform flow to be replaced by total constructive interference for a given mode, and vice versa. Even if such extreme cases do not occur, it is clear that the non-uniform mean flow can induce significant changes in the way in which the different sources interfere with each other, which then leads to large decibel changes in the *relative* noise levels, as plotted in figures 6–8. Another point is that the sharp peaks shown in figures 6–8 are characteristic of cascade noise, and by plotting out the relative effects of the various cascade contributions it can be shown that they are caused by the multiple reflections between adjacent blades, i.e. contribution (iii).

From the specimen results shown in this subsection we may conclude that the effects of blade geometry on the tonal components of rotor–stator interaction noise can be very significant.

4. Uniformly valid solution

The expressions (3.19) and (3.21) show that the plane-wave amplitudes are singular at the cut-off conditions $\theta_s^n = \alpha$ and $\theta_s^n = \alpha + \pi$ (i.e. when the modes are propagating along the front face of the cascade), and for mode angles aligned with the shadow boundaries associated with reflection of the direct field by the adjacent blade, i.e. $\theta_s^n = \pi/2$ and $\theta_s^n = \pi - \alpha$. Following the analysis of Peake & Kerschen (1995) for uniform flow, these singularities can be removed by replacing (3.21) with a uniformly valid expression for $\mathscr{F}(\theta_s^n)$. This expression will be finite for all possible mode angles, and will vanish at cut-off in order to cancel the factor $1/\sin(\theta_s^n - \alpha)$ multiplying $\mathscr{F}(\theta_s^n)$ in (3.19).

The derivation of non-singular expressions for the upstream radiation in uniform flow (Peake & Kerschen 1995) is based on a factorization of the generic Wiener–Hopf kernel for the cascade in terms of Fourier integrals, and on the steepest-descent evaluation of these integrals in the high-frequency limit. Each of the integrals possesses a pole and a saddle point, and it is explained in Peake & Kerschen (1995) that the singularities occur at the critical mode angles when the poles approach the saddle points. The Van Der Waerden (1950) method is therefore used instead of the method of steepest descent to obtain a uniformly valid expansion of the Wiener–Hopf factors. In order to include mean-flow distortion in these results, one simply has to compare results (3.17)–(3.21) here with Peake & Kerschen (1995). In fact, our factor $\mathscr{F}(\theta_s^n)$ is closely related to the factor $\mathscr{L}^-(-k/\beta_\infty^2)\mathscr{L}^+(-kw\cos\theta_s^n)$ in equations (14) and (16) of Peake & Kerschen (1995), where $\mathscr{L}^-(\lambda)\mathscr{L}^+(\lambda)$ is the factorization of the Wiener–Hopf kernel $\mathscr{L}(\lambda)$ in the complex λ-plane given by relations (16) and (18) of Peake & Kerschen (1995). More precisely, we write

$$\mathscr{F}(\theta_s^n) = \mathscr{F}^-(-k/\beta_\infty^2)\mathscr{F}^+(-kw\cos\theta_s^n), \tag{4.1}$$

where the complex functions $\mathscr{F}^\pm(\lambda)$ are identical to the functions $\mathscr{L}^\pm(\lambda)$ found in Peake & Kerschen (1995), but not including contributions from the poles of the

corresponding integrals. These poles account for the direct reflections, which we have already included in the factors $E_{N,t}(\theta_s^n)$ via the step-function terms in (3.20). Once this point has been accounted for, however, it is possible to read the uniformly valid results from Peake & Kerschen (1995) straight across into the present work. The only modification which is required to account for non-uniform mean flow is to include the phase distortion of the bouncing mode (contribution iii in the previous section), which will be described below.

The factor $\mathscr{F}^-(-k/\beta_\infty^2)$ in (4.1) is never singular, and following the previous section we can write

$$\mathscr{F}^-(-k/\beta_\infty^2) = 1 - \frac{\mathrm{i}}{(kw)^{1/2}}(2^{1/2}\cos(\alpha/2)C_1 - 2^{1/2}\sin(\alpha/2)C_2 - C_3), \tag{4.2}$$

with the constants C_{1-3} given by (3.22)–(3.24) as before. The uniform expansion of Peake & Kerschen (1995) is used to correct the second term in (4.1), and we find that

$$\mathscr{F}^+(-kw\cos\theta_s^n) = \exp\left(\frac{\mathrm{e}^{\pi\mathrm{i}/4}}{2(\pi kw)^{1/2}}\sum_{m=1}^{\infty} m^{-3/2}(I_1 + I_2 + I_3)\right). \tag{4.3}$$

The terms I_{1-3} inside the summation, which depend on m and the mode index n, are

$$I_{1,2} = \exp\{\mathrm{i}mkw\Delta[1 \pm \cos(\theta_s^n - \alpha)]\}\,\mathrm{sgn}(\cos\theta_s^n \pm \cos\alpha)$$
$$\times\left[(\pi kwm)^{1/2}\mathrm{e}^{-\pi\mathrm{i}/4}w(\mathrm{e}^{\pi\mathrm{i}/4}(kwm\Upsilon_{1,2})^{1/2}) + \frac{2^{1/2}\sin\alpha}{\Delta^{1/2}|\cos\theta_s^n \pm \cos\alpha|} - \Upsilon_{1,2}^{-1/2}\right] \tag{4.4}$$

and

$$I_3 = -\exp\{2\mathrm{i}mkws + \mathrm{i}mk\delta p_2\}\,\mathrm{sgn}(\cos\theta_s^n)$$
$$\times[(\pi kwm)^{1/2}\mathrm{e}^{-\pi\mathrm{i}/4}w(\mathrm{e}^{\pi\mathrm{i}/4}(kwm\Upsilon_3)^{1/2}) + s^{-1/2}|\cos\theta_s^n|^{-1} - \Upsilon_3^{-1/2}], \tag{4.5}$$

where

$$\Upsilon_{1,2} = \Delta(1 \pm \cos\theta_s^n\cos\alpha - |\sin\theta_s^n|\sin\alpha), \tag{4.6}$$

$$\Upsilon_3 = 2s(1 - |\sin\theta_s^n|), \tag{4.7}$$

and $w(z) \equiv \exp(-z^2)\,\mathrm{erfc}(-\mathrm{i}z)$ (see Abramowitz & Stegun 1972). The modification to include the phase distortion $k\delta p_2$ of the bouncing mode (contribution iii) is now clear: the factor $\exp(2\mathrm{i}mkws)$ in the first term in (4.5) corresponds to the phase change of a ray which is reflected m times between the leading edge of a blade and the adjacent lower blade in uniform flow, so to include the flow distortion we need only introduce the additional phase term $mk\delta p_2$. The other phase distortion terms from § 3.2, $\delta kp_{1,3}$, have already been included elsewhere in our formulae, and have no bearing on the uniform expression for $\mathscr{F}(\theta_s^n)$. The occurrence of the error functions in equations (4.4) and (4.5) is of course characteristic of the uniform asymptotic description of a pole close to a saddle in a steepest descent integral (see Jones 1986, p. 718).

We briefly check the validity of our uniform expression for $\mathscr{F}(\theta_s^n)$ by considering the critical mode angles in turn. First we note that when the mode angle is not near one of its critical values, Υ_{1-3} are $O(1)$ and the error functions in (4.4) and (4.5) and the exponential in (4.3) can be expanded for large kw so that (3.21) is recovered to $O((kw)^{-1/2})$. When θ_s^n approaches the shadow boundary at $\pi/2$, the function Υ_3 vanishes, the error function in (4.5) approaches unity, and the singularities of the remaining two terms in (4.5) cancel. Consequently, I_3, the summation of I_3 over m

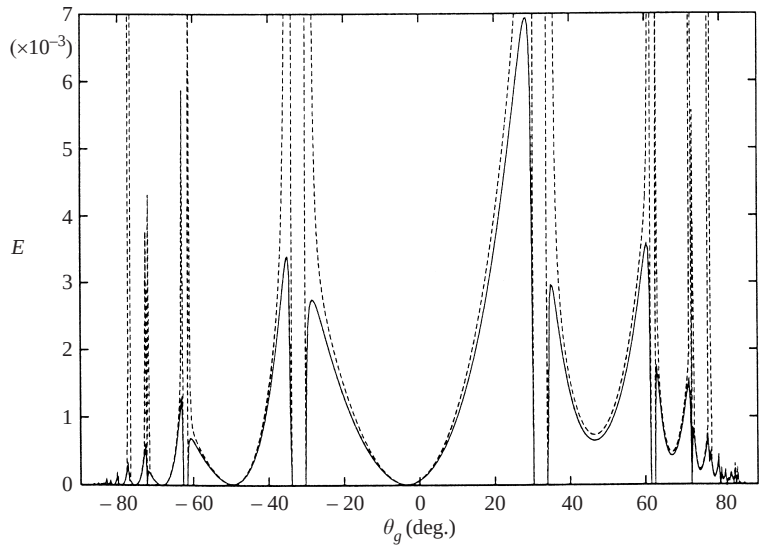

FIGURE 9. Normalized acoustic energy vs. gust angle ahead of a cascade of NACA 0006 blades at 5° angle of attack, calculated with the uniformly valid equations (solid line) and compared with the previous solution (dashed line). Relevant parameters are $\Delta_* = b$, $\alpha_* = \pi/2$, $k = 5$ and $M_\infty = 0.5$.

and hence $\mathscr{F}^+$ are well-defined. A similar structure is found in the expression for I_1 in the limit $\theta_s^n \to \pi - \alpha$, the other shadow boundary. When the mode angle approaches the cut-off condition $\theta_s^n = \alpha$, we see that $\Upsilon_2 \to 0$ and

$$I_2 \to -(\pi k w m)^{1/2} \mathrm{e}^{-\pi \mathrm{i}/4} + (2\Delta)^{-1/2} \cot \alpha. \tag{4.8}$$

It follows that $\mathscr{F}^+ \to 0$ as $\theta_s^n \to \alpha$, and that the $1/\sin(\theta_s^n - \alpha)$ singularity in (3.19) is cancelled. Similarly, I_1 is responsible for cancelling this singularity as $\theta_s^n \to \pi + \alpha$.

We now present numerical results from these uniformly valid equations. We consider a two-dimensional purely vortical gust interacting with a cascade of NACA 0006 airfoils, with angle of attack $\iota_\infty = 5°$, $k = 10$, $\sigma = 3\pi$, $\Delta_* = b$ and $\alpha_* = \pi/2$, and compare the results for the upstream energy E in figure 9. There is close agreement between the results of § 3 and § 4 when all the modes are well cut-on, but when at least one of the upstream modes comes close to cut-off the non-uniform predictions of § 3 are no longer valid. This figure demonstrates the importance of having a uniform description of the cascade response since, especially at high frequency, all the upstream modes are well cut-on over only a relatively small portion of parameter space.

Finally in this section, we compare in figure 10 our asymptotic results (specifically the uniformly valid expressions from this section) with a numerical solution. The numerical solution is taken straight from results presented by Abdelhamid & Atassi (2000), and was obtained by direct solution of Goldstein's convected wave equation (see Goldstein 1978), i.e. the same equation as has been analysed asymptotically in this paper. Further details of these computations are given in Atassi, Fang & Patrick (1993). The quantity being compared is the amplitude of the pressure associated with the nth upstream mode as a function of reduced frequency based on full-chord (i.e. $2k$), for consistency with Abdelhamid & Atassi (2000). In our notation this pressure

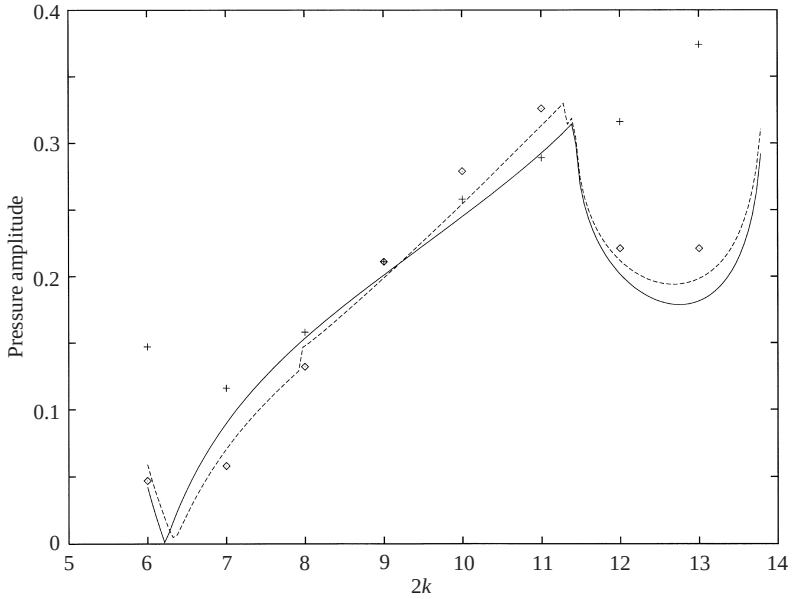

FIGURE 10. Comparison between results from our asymptotic scheme (lines) and numerical results taken from figure 7(*a*) of Abdelhamid & Atassi (2000) (symbols). We have plotted the variation of the pressure amplitude of the $n = 1$ mode upstream against $2k$, for $M_\infty = 0.3$, $\Delta_* = 2$, and $\alpha_* = \pi/4$. The gust is one-dimensional, so that $k_n = k_3 = 0$, and $A_t = A_3 = 0$, $A_n = 1$. The airfoils are at zero incidence to the upstream flow, and have zero camber; the solid line and diamond symbols are for zero-thickness flat plates, while the dashed line and cross symbols are for NACA 0012 airfoils.

amplitude is given by

$$\left| kw \cos\theta_s^n - \frac{k}{\beta_\infty^2} \right| |R_n|, \tag{4.9}$$

and the mode in question is only cut-on over the range of k values for which our asymptotic results have been plotted. The agreement seems fair, although it is noted that the parameter values used are not perhaps large enough for our asymptotics to be completely reliable. In particular, our asymptotics require both the aerodynamic reduced frequency, k, and the acoustic reduced frequency, kw, to be large. When $k_3 = 0$, $kw = kM_\infty/(1 - M_\infty^2)$, and since $M_\infty = 0.3$ in the relevant Abdelhamid & Atassi results, this second condition is not really satisfied (in figure 10 we have $0.99 < kw < 2.27$). The largest discrepancy between the two sets of results occurs for the lowest and highest frequencies shown, which is where this particular mode is close to cut-off. This perhaps indicates that the uniformly valid asymptotic solution requires higher values of kw to give an accurate result than the well-cut-on approximation given in the previous section. Even so, the agreement seen over most of the cut-on range in figure 10 is encouraging.

5. Response to turbulence spectrum

Now that a uniformly valid approximation for the cascade response to a single gust has been established, we can integrate over a spectrum of gusts to obtain the response to a full turbulence field. We will use a modification of the analysis of Hanson & Horan (1998), who consider a flat-plate cascade. One important new feature here stems from the fact that the tangential component of the gust velocity,

A_t, can generate noise in non-uniform flow, due to the interactions at the blade leading edges. This will result in contributions corresponding to cross-correlations between the normal and tangential velocity components and the auto-correlation of the tangential velocity components, in addition to the usual auto-correlation of the normal velocity which appears in Hanson & Horan (1998).

A well-known expression for the instantaneous acoustic intensity vector far upstream of the cascade, $I(\boldsymbol{x}, t)$, is given in Goldstein (1976, p. 41). The component of this intensity in the direction $\boldsymbol{n}$, where $\boldsymbol{n}$ is normal to the front face of the cascade pointing upstream, is time-averaged over a large time interval T, leading to the spatially dependent mean flux $I(\boldsymbol{x})$, which we write in the spectral form

$$\int_{-\infty}^{\infty} I_\omega(\boldsymbol{x})\,\mathrm{d}\omega. \tag{5.1}$$

Here $I_\omega(\boldsymbol{x})$ is the dimensional time-averaged energy flux per unit frequency, and it is shown by Hanson & Horan (1998) and Hanson (1997) that $I_\omega = \boldsymbol{I}_\omega \cdot \boldsymbol{n}$, where

$$\boldsymbol{I}_\omega = -\frac{2\pi \mathrm{i}\rho_\infty \omega}{T}\tilde{G}^* \left[\nabla\tilde{G} + \frac{\boldsymbol{U}_\infty}{a_\infty^2}\left(\mathrm{i}\omega\tilde{G} - U_\infty \frac{\partial \tilde{G}}{\partial x}\right)\right], \tag{5.2}$$

and $\tilde{G}(\boldsymbol{x}, \omega)$ is the time Fourier transform of the unsteady velocity potential $G'(\boldsymbol{x}, t)$.

In order to compute our results in a physically meaningful way, it proves convenient to suppose that the stator row is composed of a repeating pattern of V vanes, corresponding to the unsteady flow being periodic round an annulus at fixed radius. This means that the inter-blade phase angle σ must satisfy $\sigma = 2\pi l/V$ for any integer l. Following Hanson & Horan (1998) the sound power spectrum associated with these V blades is then found by integrating I_ω over a distance $V\Delta_*$ in the direction along the front face of the cascade and over a distance $b_*\partial R$ in the spanwise direction. Here we assume that the turbulence–cascade interaction occurs over a finite radial distance $b_*\partial R$ that is large compared with the wavelengths which dominate the acoustic field. We thus find that the dimensional sound power spectrum is

$$\Pi(\omega) = \int_0^{V\Delta_*} \int_{b\partial R} I_\omega\,\mathrm{d}z_*\,\mathrm{d}\tau, \tag{5.3}$$

where τ is the coordinate along the front face of the cascade.

The response to a single-frequency gust presented in the previous section can now be substituted into equation (5.3). Considerable simplification of equation (5.3) is possible, and full details are given in Hanson & Horan (1998) and Hanson (1997). The key feature of the Hanson & Horan (1998) result is the way it allows the inhomogeneous wake turbulence produced by an upstream rotor to be treated using results for homogeneous turbulence. This is achieved by first assuming that the rotor wakes do not decay significantly over the rotor–stator gap, and then the two integrations in (5.3) remove the spatial variations in the other two directions, so that a spectrum for homogeneous turbulence can be used in (5.3). Hanson & Horan's derivation does need to be extended to account for the contributions to the noise from the gust tangential-velocity components mentioned above, however, but this can be completed in a standard way and details need not be included. It turns out that

$$\Pi = \frac{(2\pi\epsilon U_\infty)^2 \rho_\infty b_*^3 \beta_\infty \partial R}{s\Delta k} \times \sum_{n=-\infty}^{\infty} \sum_{l} \int_{k_3} \frac{|\mathscr{F}(\theta_s^n)|^2}{\sin(\theta_s^n - \alpha)} \{\varphi_{22}|E_N|^2 + 2\,\mathrm{Re}(\varphi_{21}E_N^* E_t) + \varphi_{11}|E_t|^2\}\,\mathrm{d}k_3, \tag{5.4}$$

where φ_{ij} are the averaged turbulence wavenumber spectra, which are taken to be the idealized Liepmann model for isotropic flow (normalized by $\epsilon^2 U_\infty^2 b_*^3$), giving

$$\varphi_{ij} = \frac{2\bar{v}\Lambda^5(\delta_{ij}|\boldsymbol{\kappa}|^2 - \kappa_i\kappa_j)}{\pi^2(1+\Lambda^2|\boldsymbol{\kappa}|^2)^3} \tag{5.5}$$

in tensor notation. Here, $b_*\Lambda$ is the turbulence integral scale, $\epsilon^2 U_\infty^2 \bar{v}^2$ is the upwash intensity and

$$\boldsymbol{\kappa} = \left(k, \frac{2l\pi b_*}{Vs_*} - k\cot\alpha_*, kk_3\right) \tag{5.6}$$

is the wavenumber vector of the incident gust with respect to the axes x_*, y_* and z_* of the physical coordinate system, normalized by $1/b_*$. The second component of $\boldsymbol{\kappa}$ has been denoted by kk_n in § 3, and is now fixed by imposing periodicity around the annulus. Specifically, k_n is fixed in terms of the index l according to (3.12).

It was shown in § 3.2 that for any given k_n and k_3 (with k fixed), there is a finite number of cut-on modes with indices in the range $n_r \leqslant n \leqslant n_q$ that satisfy $|2n\pi - \sigma'| \leqslant \Lambda kw$. Conversely, for any given mode index n, there is a (non-empty) range of values of k_n (or equivalently of l) and k_3, such that this mode is cut-on. Accordingly, for every integer n, the integration and the inner summation in (5.4) are performed over only those values of k_3 and l for which the mode is cut-on. All values of n give non-zero contributions to (5.4) (the combination $l = nV$, $k_3 = 0$ is always cut-on in subsonic flow, for example), but these decay like $|n|^{-4}$ as $n \to \pm\infty$ with the wavenumber spectra φ_{ij} of the incident field, so that the outer summation in (5.4) converges.

There are two significant differences between (5.4) and the corresponding result in Hanson & Horan (1998). First, because we now take into account the distortion of the turbulence field by the mean flow and the additional sound generation due to volume sources near the leading edge, the streamwise component of the incident field now contributes to the turbulence–cascade interaction. This has resulted in the two additional terms inside the braces in (5.4) that involve E_t and the wavenumber spectra φ_{21} and φ_{11} (the function in braces is still positive definite). These are $O(k^{1/2}\delta)$ and $O(k\delta^2)$ smaller than the first term in the high-frequency, small-disturbance limits, as confirmed by comparing (3.20), (3.10) and (3.8). The other difference is in the acoustic response to the cross-stream component of the incident velocity, i.e. the term involving φ_{22}, since the interaction between the gust normal velocity and the non-uniform mean flow generates noise in addition to that produced by the momentum-blocking of the airfoil surface. The coefficient of this term, $|\mathscr{F}(\theta_s^n)E_N|^2$, is consequently different from that given by Hanson & Horan (1998). Equations (3.20), (3.24) and (4.5) show that the phase terms $k\delta p_3(\theta_s^n)$ and $k\delta p_2$ of the reflected and bouncing modes lead to interference effects that are $O(1)$ in the preferred limit $k\delta = O(1)$. These are attributed to the non-uniform mean flow and make $\mathscr{F}(\theta_s^n)$, E_N and E_t significantly different from their flat-plate, zero-incidence counterparts. However, we do note that the gust drift $k\delta g_l$ and the phase distortion of the direct acoustic field $k\delta p_1$ cancel out in (5.4), essentially because of taking the time-average, confirming our statement in § 2 that only the strength of the leading-edge flow is required from the steady-flow calculations. Of course, although the turbulence far upstream of the stator has been represented as being homogeneous once the averaging in (5.3) has been completed, the non-uniform steady flow round the cascade distorts this turbulence as it convects downstream, modifying the noise through the presence of the drift phase factor $k\delta g_l$. It is interesting that this distortion does not affect our time-averaged measures of the

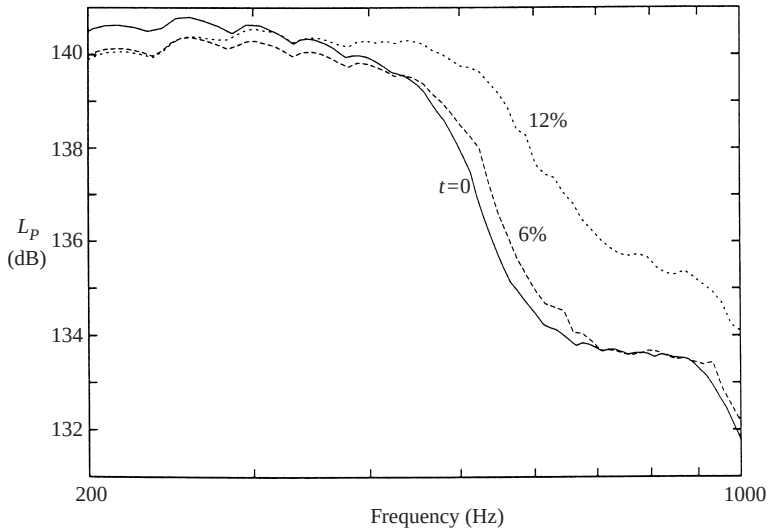

FIGURE 11. Noise spectrum for a cascade of uncambered airfoils at zero angle of attack, with thicknesses $t = 0$, 6, 12% of chord. Here $M_\infty = 0.5$.

noise, but this is no doubt a consequence of the asymptotic limit $\delta \ll 1$, leading to only weakly non-uniform mean flow. For more strongly non-uniform mean flow, for instance produced by blades with $O(1)$ camber, the distortion of the turbulence would lead to a more significant effect than the simple phase distortion found here, which could in turn then feature in our time-averaged measures of the noise.

We present results in decibels using the definition

$$L_P = 10 \log_{10} \left(\frac{2\Pi}{10^{-12}\,\mathrm{W}} \right) \tag{5.7}$$

for the power level L_P, with realistic values $V = 25$, $b_* = 0.2\,\mathrm{m}$, $\alpha_* = 60^\circ$, $\Lambda_* = 1.6 b_*$, turbulence intensity $\bar{v}^2 = 0.0001 U_\infty^2$, and turbulence integral lengthscale $\Lambda = 0.5 b_*$. For this choice of integral lengthscale it should be noted that part of the turbulent energy is in the low to moderate frequency range, where our asymptotics lose validity. However, it could be expected that the effects of the blade geometry are less important at low frequency.

In figure 11 we consider NACA 00XX blades at zero angle of attack with varying thicknesses at $M_\infty = 0.5$, and we find that an increase in thickness is seen to increase the spectrum level, particularly for the highest frequencies, by 2–3 dB. A similar comparison at $M_\infty = 0.3$ between a cascade of flat plates at zero incidence and a cascade of NACA airfoils with 5% camber, 6% thickness and 5° angle of attack is made in figure 12. Here, the difference is of the order of only 1 dB. It should be noted that in dimensionless terms the lowest frequencies shown in figures 11 and 12 are $k \approx 1.23$ and $k \approx 1.48$ respectively. This means that the lowest frequencies shown in the figures are perhaps at too low a value of k for our asymptotics to be accurate there. However, for these lower frequencies one would expect there to be rather little effect from the non-uniform flow anyway, so that the real question of interest is the effect of the non-uniform flow on the parts of the incident spectrum at the higher frequencies shown in these figures.

The effects of blade geometry on broadband noise are seen here to be lower than

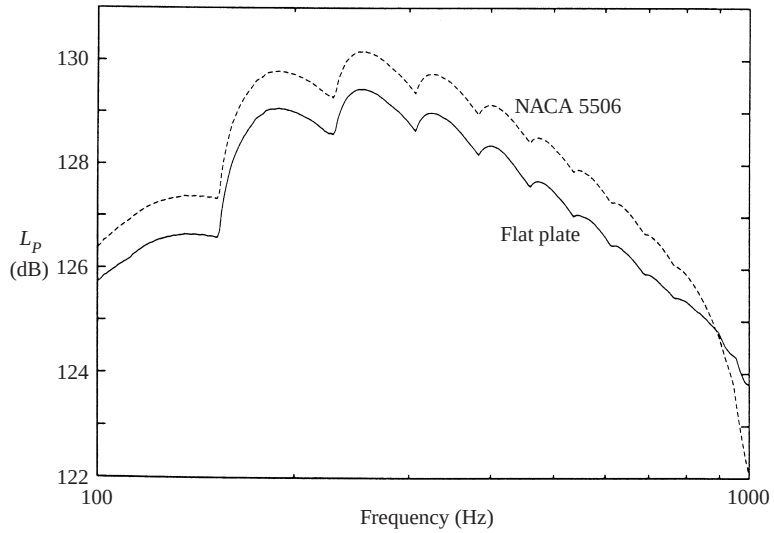

FIGURE 12. Noise spectrum for a cascade of NACA 5506 airfoils at 5° angle of attack compared with that for a cascade of flat-plate blades at zero angle of attack. $M_\infty = 0.3$.

might have been expected in the light of the results presented in § 3 for single gusts. Our hypothesis is that the reason for this lies in the fact that the broadband radiation spectrum is given, as in equation (5.4), as an integral over spanwise wavenumber k_3 (specifically over the range of values of k_3 for which at least one mode is cut on upstream of the cascade). This is in contrast to the single-gust results, which are all for a single value of k_3. We have already emphasized the idea that for large k the non-uniform flow has the effect of inducing $O(1)$ phase changes on the various components of the noise. For example, we pointed out at the end of § 3 that the interference between a given leading edge and its image source in the adjacent blade is modified by the $O(1)$ phase correction $k\delta p_3$, and depending on the precise value of p_3 this phase change either leads to interference which is more constructive than the case $\delta = 0$ (in which case the noise increases compared to the $\delta = 0$ case), or the phase change leads to interference which is more destructive (in which case the noise decreases). Now the quantity p_3 depends on the spanwise wavenumber k_3 quite strongly; p_3 depends on the mode angle θ_s^n (equation (3.16)), which itself depends on w (equation (3.18)) and in turn on k_3 (equation (3.4)). Our idea is that as k_3 varies through the integration range in equation (5.4), p_3 will also vary, and that the contributions to the integral in which the value of p_3 tends to increase the sound above the $\delta = 0$ level will tend to, at least partially, cancel contributions for which the value of p_3 tends to reduce the sound below the $\delta = 0$ level. Of course, for a single gust, with a single value of k_3, this cancellation cannot occur. This may then explain why the very largest changes to the single-gust results when non-uniform flow is introduced, as observed for some parameter values in § 3, are not seen here for broadband noise.

One final point to note is that experimental and theoretical studies of turbulence interacting with isolated airfoils (Paterson & Amiet 1976, 1977) also show that the angle of attack has only a relatively small effect on broadband noise levels. The explanation given in Paterson & Amiet (1976) is that, at least for incompressible flow (and therefore at low frequency), it is the component of the gust normal to the blade

chord which generates the unsteady response. This means that at zero incidence it is only the gust velocity normal to the upstream flow which produces unsteady lift. But, at non-zero incidence the gust velocity parallel to the upstream flow has a non-zero component normal to the blade chord, which provides an additional unsteady lift proportional to angle of attack, and which is therefore small (see Horlock 1969). This is in fact included, at high frequency, within our current analysis, via the terms involving E_t in equation (5.4). Paterson & Amiet's argument could be applied to a cascade as well, but only at low frequency where the distortion effects of the non-uniform flow would be small. At the higher frequencies, we have already seen in § 3 that the single-gust response changes very markedly with changing the properties of the non-uniform steady flow. We then suggest that the suppression of the non-uniform flow effects on higher-frequency broadband noise in a cascade could be due instead to the sort of interference effects described in the previous paragraph.

6. Concluding remarks

In this paper we have presented an asymptotic scheme to predict cascade noise with non-uniform flow, by extending earlier results for gust–cascade interaction (Peake & Kerschen 1997) to include the effects of camber and thickness. A novel method of calculating the steady cascade flow has resulted in a closed-form expression for the leading-edge singularity, which is easily included in the unsteady problem. Indeed, we emphasize that the coefficient of this singularity is the only quantity from the steady flow which needs to be calculated in order to predict time-averaged noise levels in our model. Formulae that are valid near modal cut-off have been derived using the results of Peake & Kerschen (1995). This gust response is then fed into a modification of the Hanson & Horan (1998) scheme for turbulence–cascade interaction.

When only single harmonic gusts are considered, the noise produced by blades with non-zero thickness and angle of attack can be very different (by up to 10 dB) from the corresponding flat-plate results. This can be attributed primarily to the $O(k\delta)$ phase distortions induced by non-uniformities in the mean flow. To a lesser extent, additional terms in the amplitudes of the leading-edge ray fields that result from the large mean-flow gradients (i.e. volume source terms and terms that result from steady–unsteady flow interactions) also affect the upstream acoustic response. This all means that the blade geometry is likely to have a significant effect on the tonal components of rotor–stator interaction noise. However, these effects average out somewhat when the gust responses are integrated over the full incident turbulence spectrum. Even so, changes of the order of 2 dB can be observed in the broadband acoustic spectrum when blade geometry is included, which is certainly significant in a practical context.

I. E. gratefully acknowledges the financial support provided by the European Commission under the Training and Mobility of Researchers programme. The latter stages of this work were supported by the Engineering and Physical Sciences Research Council under Contract GR/M21638.

REFERENCES

Abdelhamid, Y. A. & Atassi, H. M. 2000 Effects of blade shape and loading on the acoustic radiation of a casade. *AIAA Paper* 2000-2093-CP.

Abramowitz, M. & Stegun, I. A. 1972 *Handbook of Mathematical Functions*. Dover.

Amiet, R. K. 1976 High-frequency thin-airfoil theory for subsonic flow. *AIAA J.* **14**, 1076–1082.

Atassi, H. M. & Grzedzinski, J. 1989 Unsteady disturbances of streaming motions around bodies. *J. Fluid Mech.* **209**, 385–403.

Atassi, H. M., Fang, J. & Patrick, S. 1993 Direct calculation of sound radiated from bodies in nonuniform flows. *Trans. ASME: J. Fluids Engng* **115**, 573–579.

Atassi, H. M., Subramaniam, S. & Scott, J. R. 1990 Acoustic radiation from lifting airfoils in compressible subsonic flow. *AIAA Paper* 90-3911.

Batchelor, G. K. & Proudman, I. 1954 The effect of rapid distortion of a fluid in turbulent motion. *Q. J. Mech. Appl. Maths* **1**, 83.

Carter, A. D. S. & Hughes, H. P. 1946 A theoretical investigation into the effect of profile shape on the performance of aerofoils in cascade. *Tech. Rep.* 2384. ARC R&M.

Evers, I. 1999 Sound generation in turbomachinery flow. PhD thesis, University of Cambridge.

Evers, I. & Peake, N. 2000 Noise generation by high-frequency gusts interacting with an airfoil in transonic flow. *J. Fluid Mech.* **411**, 91–130.

Goldstein, M. E. 1976 *Aeroacoustics.* McGraw-Hill.

Goldstein, M. E. 1978 Unsteady vortical and entropic disturbances of potential flows round arbitrary obstacles. *J. Fluid Mech.* **89**, 433–468.

Goto, A. & Shirakura, M. 1982 Potential flow analysis of an arbitrary cascade using a conformal transformation into a row of circular cylinders. *Bull. JSME* **208**, 1498–1505.

Grammel, R. 1917 *Die Hydrodynamischen Grundlagen des Fluges.* Braunschweig: F. Vieweg.

Hall, W. S. & Thwaites, B. 1962 On the calculation of cascade flows. *Tech. Rep.* 618. ARC CP.

Hanson, D. B. 1997 Quantification of inflow turbulence for prediction of cascade broadband noise. *Sound and Vibration, 5th Intl Congress, Adelaide, Australia*, Paper 990544.

Hanson, D. B. & Horan, K. P. 1998 Turbulence/cascade interaction: spectra of inflow, cascade response, and noise. *AIAA Paper* 98-2319.

Horlock, J. H. 1969 Fluctuating lift forces on airfoils moving through transverse and chordwise gusts. *Trans. ASME: J. Basic Engng* **90**, 494–500.

Houghton, E. L. & Carruthers, N. B. 1982 *Aerodynamics for Engineering Students*, 3rd Edn. Edward Arnold.

Kerschen, E. J. & Myers, M. R. 1986 Transformation of the equation governing disturbances of a two-dimensional compressible flow. *AIAA J.* **19**, 1367–1370.

Koch, W. 1971 On the transmission of sound waves through a blade row. *J. Sound Vib.* **18**, 111–128.

Jones, D. S. 1986 *Acoustic and Electromagnetic Waves.* Oxford University Press.

Lewis, R. I. 1991 *Vortex Element Methods for Fluid Dynamic Analysis of Engineering Systems.* Cambridge University Press.

Mani, R. & Horvay, G. 1970 Sound transmission through blade rows. *J. Sound Vib.* **12**, 59–83.

Martensen, E. 1959 Berechnung der Druckverteilung an Gitterprofilen in ebener Potentialstromung mit einer Fredholmschen integralgleichung. *Arch. Rat. Mech. Anal.* **3**, 235–270.

Martensen, E. 1971 The calculation of pressure distribution on a cascade of thick airfoils by means of fredholm integral equations of the second kind. *Tech. Rep.* F-702. NASA TT.

Mellor, G. L. 1959 An analysis of axial compressor cascade aerodynamics. *Trans. ASME: J. Basic Engng* **81**, 361–378.

Merchant, W. & Collar, A. R. 1941 Flow of an ideal fluid past a cascade of blades (part II). *Tech. Rep.* 1893. ARC R&M.

Myers, M. R. & Kerschen, E. J. 1995 Influence of incidence angle on sound generation by aerfoils interacting with high-frequency gusts. *J. Fluid Mech.* **292**, 271–304.

Myers, M. R. & Kerschen, E. J. 1997 Influence of camber on sound generation by airfoils interacting with high-frequency gusts. *J. Fluid Mech.* **353**, 221–259.

Paterson, W. & Amiet, R. K. 1976 Acoustic radiation and surface pressure characteristics of an airfoil to incident turbulence. *NASA Contractor Rep.* CR-2733.

Paterson, W. & Amiet, R. K. 1977 Noise and surface pressure response of an airfoil to incident turbulence. *J. Aircraft* **14**, 729–736.

Peake, N. 1992 The interaction between a high-frequency gust and a blade row. *J. Fluid Mech.* **241**, 261–289.

Peake, N. & Kerschen, E. J. 1995 A uniform asymptotic approximation for high-frequency unsteady cascade flow. *Proc. R. Soc. Lond.* A **449**, 177–186.

Peake, N. & Kerschen, E. J. 1997 Influence of mean loading on noise generated by the interaction of gusts with a flat-plate cascade: upstream radiation. *J. Fluid Mech.* **347**, 315–346.

Robinson, A. & Laurmann, J. A. 1956 *Wing Theory*. Cambridge University Press.

Schlichting, H. 1955 Berechnung der reibungslosen inkompressiblen Strömung für ein vorgegebenes ebenes Schaufelgitter. *V.D.K. Forschungshaft* **447**.

Smith, S. N. 1972 Discrete frequency sound generation in axial flow turbomachines. *Brit. Aeronaut. Res. Coun. R&M* 3709.

Tsai, C. T. & Kerschen, E. J. 1990 Influence of airfoil nose radius on sound generated by gust interactions. *AIAA Paper* 90-3912.

Van Der Waerden, B. L. 1950 On the method of saddle points. *App. Sci. Res.* B2.

Verdon, J. M. 1993 Review of unsteady aerodynamic methods for turbomachinery aeroelastic and aeroacoustic applications. *AIAA J.* **31**, 235–250.